European Journal of Radiology Open 3 (2016) 22–30

Contents lists available at ScienceDirect

European Journal of Radiology Open

journal homepage: www.elsevier.com/locate/ejro

Role of 3T multiparametric-MRI with BOLD hypoxia imaging for diagnosis and post therapy response evaluation of postoperative recurrent cervical cancers

Abhishek Mahajan[a,b,*], Reena Engineer[c], Supriya Chopra[c], Umesh Mahanshetty[c], S.L. Juvekar[a], S.K. Shrivastava[c], Naresh Desekar[a], M.H. Thakur[a]

[a] Department of Radiodiagnosis and Imaging, Tata Memorial Centre, Mumbai 400012, India
[b] Department of Imaging Sciences and Biomedical Engineering, Kings College London, UK
[c] Department of Radiation-Oncology, Tata Memorial Centre, Mumbai 400012, India

ARTICLE INFO

Article history:
Received 17 September 2015
Accepted 21 November 2015
Available online 12 December 2015

Keywords:
Hypoxia
MRI
Cervical cancer
BOLD
Neoplasia
Molecular
Hypoxia imaging
Image guided radiotherapy
Radiobiology
Molecular imaging
Intensity modulated radiotherapy (IMRT)
MR-spectroscopy
MR-functional imaging
Blood oxygen level dependent(BOLD) imaging
MR-diffusion/perfusion

ABSTRACT

Objectives: To assess the diagnostic value of multiparametric-MRI (MPMRI) with hypoxia imaging as a functional marker for characterizing and detecting vaginal vault/local recurrence following primary surgery for cervical cancer.
Methods: With institutional review board approval and written informed consent 30 women (median age: 45 years) from October 2009 to March 2010 with previous operated carcinoma cervix and suspected clinical vaginal vault/local recurrence were examined with 3.0T-MRI. MRI imaging included conventional and MPMRI sequences [dynamic contrast enhanced (DCE), diffusion weighted (DW), 1H-MR spectroscopy (1HMRS), blood oxygen level dependent hypoxia imaging (BOLD)]. Two radiologists, blinded to pathologic findings, independently assessed the pretherapy MRI findings and then correlated it with histopathology findings. Sensitivity, specificity, positive predictive value, negative predictive value and their confidence intervals were calculated. The pre and post therapy conventional and MPMRI parameters were analyzed and correlated with response to therapy.
Results: Of the 30 patients, there were 24 recurrent tumors and 6 benign lesions. The accuracy of diagnosing recurrent vault lesions was highest at combined MPMRI and conventional MRI (100%) than at conventional-MRI (70%) or MPMRI (96.7%) alone. Significant correlation was seen between percentage tumor regression and pre-treatment parameters such as negative enhancement integral (NEI) ($p = 0.02$), the maximum slope ($p = 0.04$), mADC value ($p = 0.001$) and amount of hypoxic fraction on the pretherapy MRI ($p = 0.01$).
Conclusion: Conventional-MR with MPMRI significantly increases the diagnostic accuracy for suspected vaginal vault/local recurrence. Post therapy serial MPMRI with hypoxia imaging follow-up objectively documents the response. MPMRI and BOLD hypoxia imaging provide information regarding tumor biology at the molecular, subcellular, cellular and tissue levels and this information may be used as an appropriate and reliable biologic target for radiation dose painting to optimize therapy in future.

1. Introduction

Cervical carcinoma is the third most common gynecologic malignancy. Approximately 85% of the global burden is from developing countries, where it accounts for 13% of all female cancers [1]. Even though there have been significant advances in surgical techniques, radiotherapy, and chemotherapy, still approximately 30% of patients with invasive cervical carcinoma die as a result of residual or recurrent disease [2].

Survival has improved with advances in the management of these patients with additional radiation therapy or chemotherapy,

Abbreviations: MPMRI, multiparametric-MRI; DCE, dynamic contrast enhanced; DWI, diffusion weighted imaging; 1HMRS, proton magnetic resonance spectroscopy; BOLD, blood oxygen level dependent; NEI, negative enhancement integral; ADC, apparent diffusion coefficient; PD-IDEAL, proton density iterative decomposition of water and fat with echo asymmetric and least-squares estimation.

* Corresponding author at: Dr. Abhishek Mahajan, MBBS, MD, Fellowship Cancer Imaging, MRes, Room no. 120, Department of Radiodiagnosis, Tata Memorial Hospital, Dr E Borges Road, Parel, Mumbai 400012, India.
E-mail addresses: abhishek.mahajan@kcl.ac.uk, drabhishek.mahajan@yahoo.in (A. Mahajan).

http://dx.doi.org/10.1016/j.ejro.2015.11.003

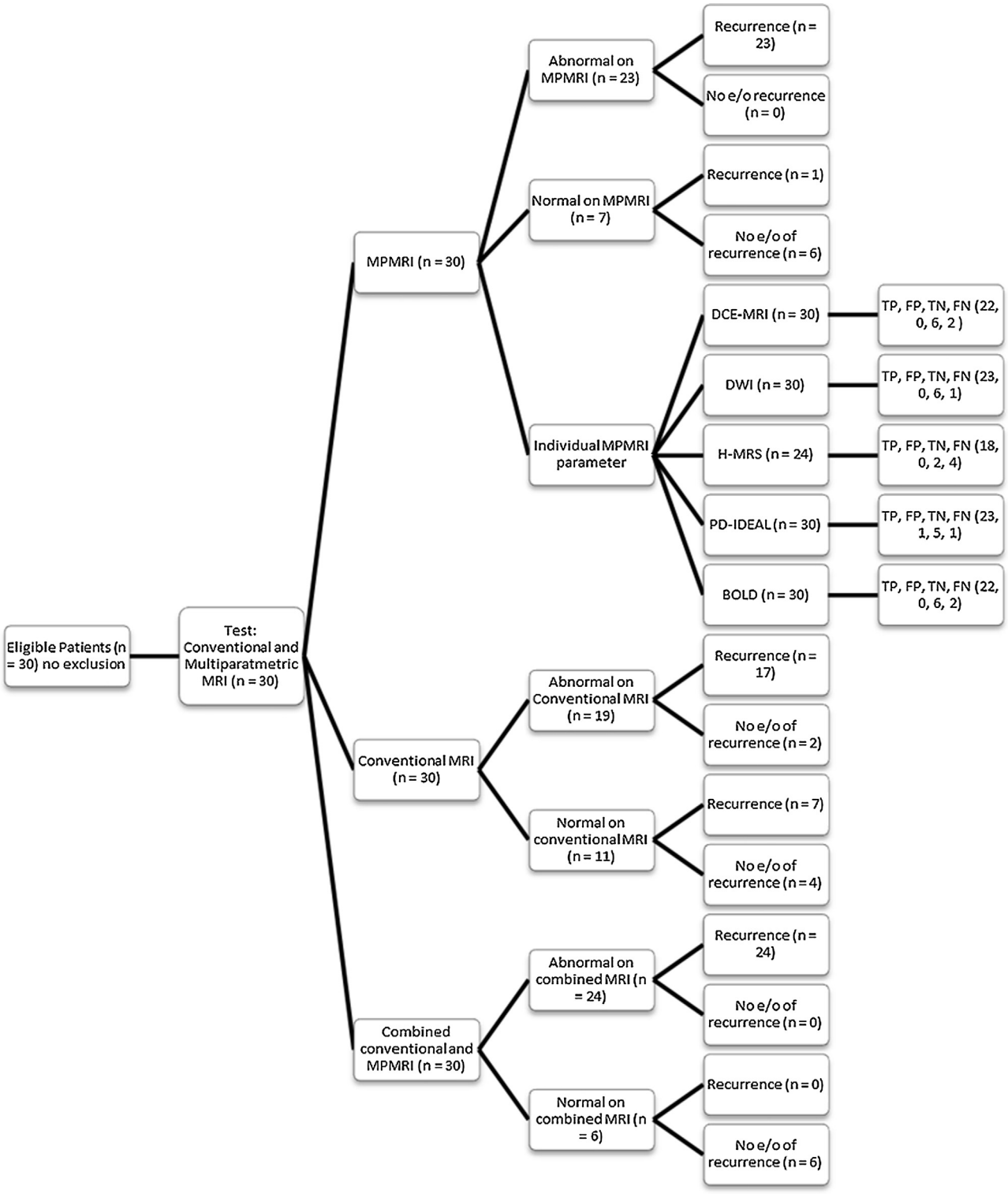

Fig. 1. Diagnostic flowchart of patient population.

still early detection of recurrent cervical carcinoma is imperative. The follow-up after primary therapy is usually performed with clinical examination and imaging {computed tomography (CT) or magnetic resonance imaging (MRI)} [3,4]. Because of the wide availability and certain advantages, such as rapid acquisition time, lack of bowel motion artifact, and fewer contraindications than MRI, CT is most widely used for follow up and is a diagnostic tool for detection of recurrence [3]. However, the value of CT in differentiating recurrence from postoperative changes/post radiation fibrosis is limited [3,4]. Fewer studies exist in literature to confirm the usefulness of MRI over CT for diagnosis of recurrent cervical carcinoma and differentiating it from radiation fibrosis [3,4,5].

Combined anatomic and physiologic information at multiparametric MRI (MPMRI) with BOLD hypoxia imaging makes it an interesting tool for detection and grading of tumors. MPMRI has been extensively used in diagnosing and characterizing pro-

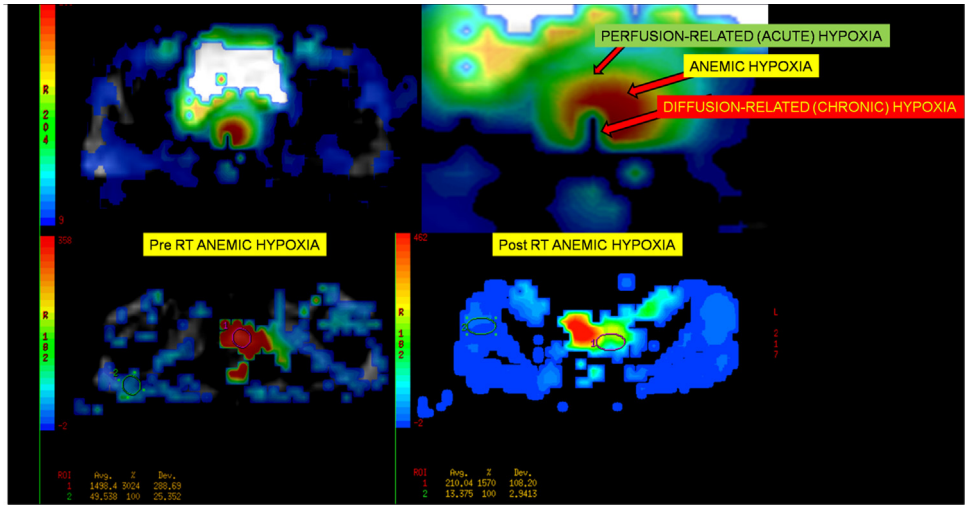

Fig. 2. (a) BOLD post-processing of the lesion which shows a rainbow color spectrum where central red spectra represented the highest R2* levels, indicating the maximum concentration of deoxyhaemoglobin suggestive of diffusion related chronic hypoxia, with intermediate yellow spectra representing relatively lower R* levels than that of red corresponding to anemic hypoxic zone and outer most green spectra suggestive of acute perfusion related hypoxia. Blue spectra represented the lowest R2* levels, indicating the minimum concentration of deoxyhaemoglobin. (b) Pre and post therapy comparison of the hypoxic fraction in the recurrent tumor is shown with significant regression in the central chronic diffusion related hypoxic fraction zone and conversion of the tumor biology from chronic to acute perfusion and anemic zone zones having lower levels of deoxyhaemoglobin levels, suggestive of response to therapy. (For interpretation of the references to colour in this figure legend, the reader is referred to the web version of this article.)

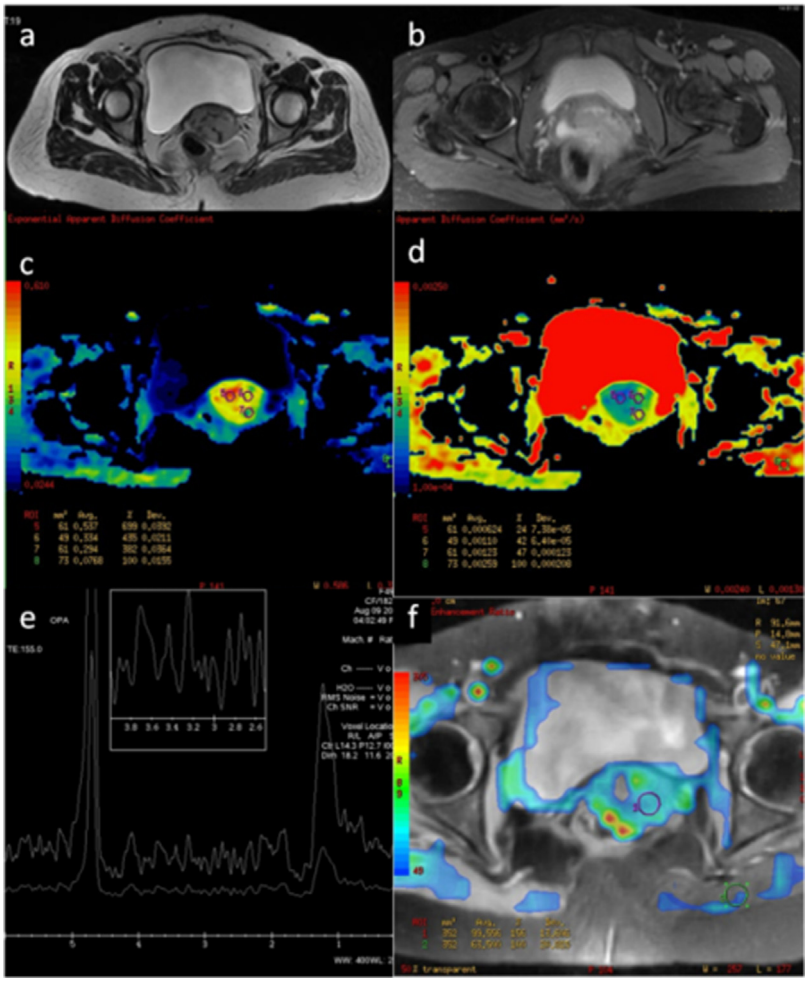

Fig. 3. Case 1: Histopathological confirmed vault recurrence. On conventional MRI showing Iso-hypointense on T2 W image (a) with mild post contrast enhancement on LAVA sequence (b). On DWI there was restricted diffusion (c) with low ADC value (d), on MRS elevated choline at 3.2 ppm (e) and on DCE-MRI area of Hhyperperfusion was noted (f).

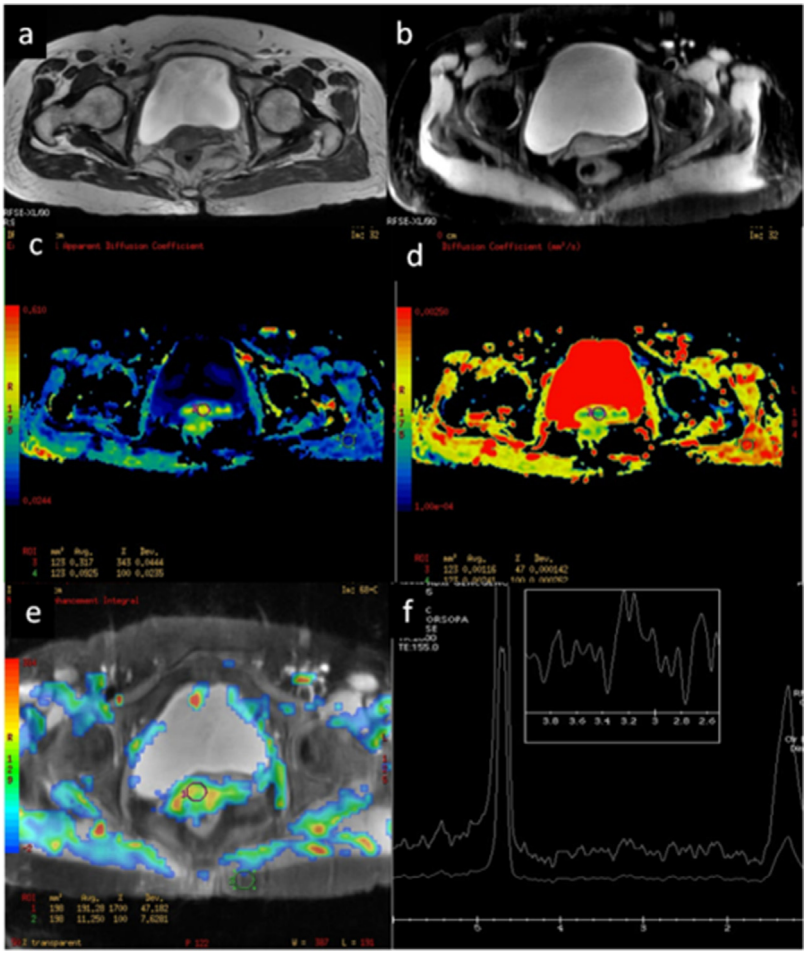

Fig. 4. Case 2: Histopathological confirmed vault recurrence. On conventional MRI showing Iso-hypointense on T2 W image (a) with heterogeneous post contrast enhancement on LAVA sequence (b). On DWI there was restricted diffusion (c) with low ADC value (d), on BOLD image area of two small hypoxic foci were noted represented by red color, the rest of the tissue was relatively well oxygenated represented by green and blue colors (e) and on MRS elevated choline at 3.2 ppm (f). (For interpretation of the references to colour in this figure legend, the reader is referred to the web version of this article.)

static cancer and post radical prostatectomy recurrences. Diffusion weighted imaging has shown promising results in evaluating primary cervical cancer as well as postoperative vault/local recurrences and is found to be biomarker for predicting response to therapy in both scenarios. Similarly Dynamic contrast enhanced (DCE) MR Imaging and 1H MR spectroscopy (1H MRS) has also been investigated as a potential imaging biomarker for both primary and postoperative recurrent cervical cancers.

Literature on the role of combined use of these functional biomarker parameters constituting MPMRI with hypoxia imaging in diagnosing vaginal vault/local recurrence in postoperative carcinoma cervix is sparse and discordant and the diagnostic relevance of MPMRI and hypoxia imaging is underutilized. So we aimed to evaluate the role of MPMRI with hypoxia imaging as a functional marker for the detection of vaginal vault/local recurrence following primary surgery for cervical cancer. The findings were compared to the final Histopathological diagnosis. The objectives of the study were:

1. To characterize suspected postoperative vaginal vault/local recurrent cervical cancer lesions on MPMRI with BOLD hypoxia imaging.
2. To assess the diagnostic value of MPMRI and hypoxia imaging as functional marker to determine the tumor recurrence in postoperative cases of cervical cancer.

2. Materials and methods

2.1. Study design and population

The study was approved by institutional review board and the hospital ethics committee. From Oct 2009 to March 2010, 45 consecutive women with previously operated carcinoma cervix with suspected vault/local recurrence were recruited in the study. Patients who had a final histopathology diagnosis and all the required MPMRI and hypoxia imaging sequences were included in the analysis and patients with no previous surgical details, without histopathological diagnosis and who were lost to follow up were excluded from the final analysis. The prospective radiologic-pathologic database included 30 patients which were included for the final analysis. All patients underwent baseline CT and MPMRI and were followed up for two years. Of the 30 post operated carcinoma cervix patients with suspected clinical vaginal vault/local recurrence, 24 had histologically confirmed recurrent lesions (Fig. 1). The median age at recurrence was 45 years (range 34–72 years).

There were four cases of benign fibrotic lesion with inflammatory changes and two had fibrotic changes with superadded local infection. The cases with with superadded infection were followed-up with MPMRI imaging.

Of the 24 recurrent cases, 16 (67%) had squamous carcinoma, 6 (25%) had adenocarcinoma and 2 (8%) had adenosqaumous

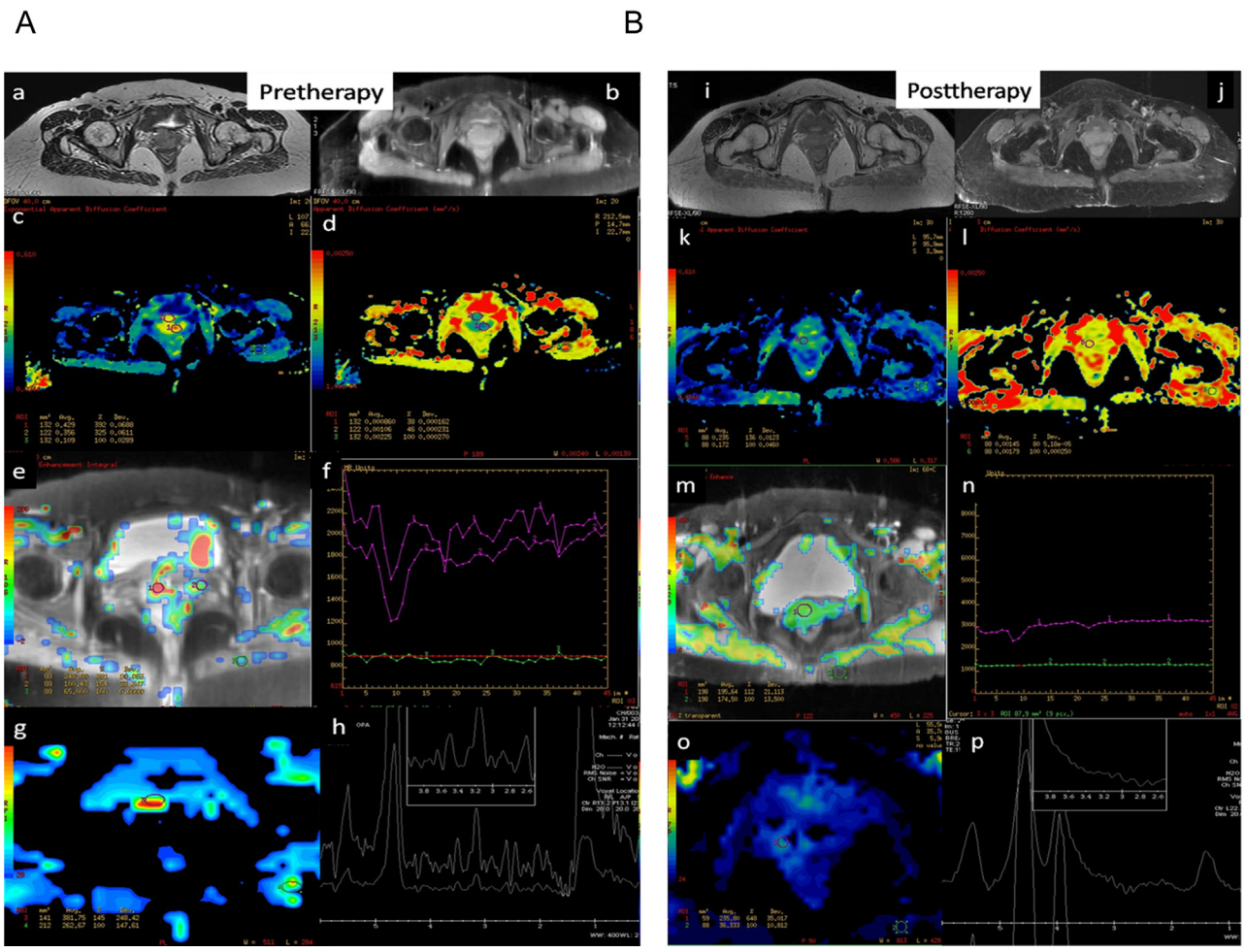

Fig. 5. (A and B). Case 3: Conventional and MPMRI in a case of vault recurrence: pre and post therapy imaging findings. Conventional and MPMRI comparison showed that there was a mild interval regression of tumor volume with no significant change in the enhancement (a, b and i, j). On DWI images there was interval regression on the restricted component with significant increase in the ADC values (c, d and k, l). On DCE-MRI there is a significant regression of the perfusion with a significant decrease in the slope of enhancement (e, f and m, n). On BOLD sequence there was a small central core of hypoxia which on follow up showed significant regression in the chronic hypoxic fractions and near normal oxygenation (g and o). On MRS the choline peak noted at 3.2 peak was absent in the follow up MRS (h and p). All these findings were suggestive of response to therapy, predicted at the molecular level with not much change in the morphology of the lesion.

Table 1
MR imaging parameters for conventional and MPMRI sequences.

Sequence	TE	TR	Slice thickness	Slice gap	Field of view	Matrix	NEX	Band width	Flip angle	Echo train length
AXIAL T1	10	400	3	1	40	320 × 224	4	41.67	–	5
AXIAL T2	100	5000	3	1	40	320 × 224	4	41.67	–	21
AXIAL T2CUDE 3D	20	2000	3	1	40	256 × 256	1	41.67	–	40
SAGITTAL T2	100	5000	3	1	24	256 × 256	4	41.67	–	19
CORONAL T2	6	5000	3	1	32	256 × 256	4	31.25	–	19
BOLD#	30	2000	3	1	40	256 × 256	1	–	90	–
DWI *b* value 0 and 700	100	6000	3	1	40	256 × 256	8	–	–	–
PD-IDEAL	30	4000	3	1	40	256 × 265	2	83.33	–	10
DCE	10	1600	3	1	40	256 × 256	1	–	80	–
LAVA + C@	2.3	4.7			40	256 × 256	1	62.5	15	–
AXIAL T1 + C	10	1000	3	1	40	320 × 224	4	41.67		5
CORONAL T1 + C	10	400	3	1	32	256 × 256	4	41.67	80	
SAGITAL T1 + C	10	600	3	1	24	256 × 256	4	41.67		5
MRS[a]	155	2000					32			

$T2^{*}$-weighted gradient-echo imaging was performed for BOLD imaging on normal breathing.
@: Intravenous injection of Gadobenate dimeglumine (MultiHance; Bracco Imaging) administered at a rate of 2 ml/s and at a dose of 0.1 mmol/kg of body weight followed by 20 ml saline flush (0.9%) by using a power injector.
[a] 1H-MRS breast spectroscopy sequence named MR BREASE which is a point-resolved spin-echo sequence with regional saturation bands for outer volume suppression was used for MRS.

carcinoma. The median time interval from baseline MPMRI to the histopathology confirmation was 7.5 days (range 1–12 days). Of the 24 patients, 12 patients had an additional post-chemo-radiotherapy MPMRI, the mean interval between the baseline MPMRI scan and the 1st port therapy MPMRI scan was 180 days.

2.2. MR imaging methodology and data analysis

MPMRI protocol was standardized in all cases. MRI was performed on the 3.0-T system (GE Signa 3.0T HDx, GE Healthcare, Milwaukee, WI) using a torso phased-array with the patient in the supine position. We used approximately 60 ml of bacteriostatic ultrasound jelly to distend the vaginal lumen. The various imaging parameters are summarized in Table 1. After determining the anatomic orientation of the vault/local was determined on the localizer images, fast spin-echo T2-weighted images were obtained in three orthogonal plane. After baseline acquisitions, dynamic contrast-enhanced (DCE) images were obtained after administration of a bolus Intravenous injection of Gadobenate dimeglumine (MultiHance; Bracco Imaging) administered at a rate of 2 ml/s and at a dose of 0.1 mmol/kg of body weight followed by 20 ml saline flush (0.9%) by using a power injector.

For assessment of MPMRI functional sequences and BOLD hypoxia imaging, data were transferred to a GE Advantage Workstation, and manually drawn regions of interest (ROIs) were analyzed using Advantage Windows, version 4.2.3, GE Healthcare. The results of MPMRI were individually analyzed for each functional MRI sequence.

MR imaging data sets were evaluated by two radiologists with 5 and 14 years of experience in gynecology MR imaging, respectively. MR imaging data sets of T1-weighted and T2-weighted MR images, PD-IDEAL imaging, three plane post contrast T1-weighted images, apparent diffusion coefficient (ADC) maps from Diffusion weighted imaging (DWI), MR spectroscopic images, dynamic contrast-enhanced MR images and BOLD (Blood oxygen level dependent) images were assessed and both reviewers were blinded to histopathology findings. The lesion was delineated both the radiologists independently, in the axial T2-weighted images and the same was transferred from the T2-weighted image series to the series from the DWI and DCE-MRI for coordinated mapping of the disease.

Based on the MR signal intensity pattern the lesions were categorized, into three categories:

1. Normal (no focal soft-tissue nodule);
2. Indeterminate (soft-tissue nodule hypointense or isointense to muscle on T1-weighted sequences and mildly hyperintense to muscle on T2-weighted sequences);
3. Recurrent (soft-tissue nodule hypointense on T1-weighted sequence and markedly hyperintense or heterogeneous on T2-weighted sequences).

For Proton Density Iterative decomposition of water and fat with echo asymmetry and least-squares estimation (PD-IDEAL) sequences four set of processed images were obtained and these were WATER only, FAT only, IN phase and OUT of phase images.

DWI analysis was done by quantitative analysis of the data acquired from DWI and pixel-by-pixel ADC maps were derived using advantage Windows, version 4.2.3, GE Healthcare. DWI Images were identified and matched to enable measurements at the same anatomic levels and the lesions were localized on the $b = 0$ s/mm^2 (i.e. b_0) images. Obvious areas of air or fluid from central ulceration were excluded and the findings on both the eADC and mADC maps were analysed both qualitatively and quantitatively (Table 2). Region of interest (ROI) were drawn manually avoiding negative pixels and subsequent measurements on the anatomically corresponding ADC maps were generated on a pixel-by-pixel basis using b values of 0 and 700 s/mm^2 ($ADC_{b0-1000}$) on dedicated workstation using the proprietary, manufacturer provided software (ADW 4.4). Of the various ROI placed in the lesion, the lowest ADC value obtained was recorded.

The DCE-MRI series were analyzed on a voxel-by-voxel basis by using the arterial input function and presented as histograms for each time point in the dynamic series. Necrosis within the tumor volume, if present, was included in the delineation. The first-pass DCE method was used to obtain a time-signal intensity (SI) DCE curve. The perfusion parameter calculated was the negative enhancement integral (Area under the curve: relative blood volume).

We used BREASE GE software to obtain robust Choline signals for MR-spectroscopy analysis. A cubed volume voxel was placed in the region of interest of critical importance. Total choline containing resonance (tCho) at 3.2 ppm in spectra was qualitatively determined.

Post processed BOLD maps were generated and ROIs were marked in the region of interest using an ROI tool to calculate R2* levels (Fig. 2). Pre and post therapy hypoxic fraction was compared in all the 24 recurrences treated that were treated with radiotherapy.

2.3. Treatment and follow-up assessment of response

Patients with histopathological diagnosis of recurrence received image guided intensity modulated radiotherapy (IG-IMRT) with concomitant chemotherapy. IG-IMRT schedule consisted of 50 Gy/25 fractions delivered over 5 weeks along with concurrent weekly cisplatin (40 mg/m^2). Response assessment and brachytherapy preplanning MPMRI were performed within a week of completing IG-IMRT. Subsequently, all patients underwent template guided high dose pelvic interstitial brachytherapy (20 Gy/5 #/3 days).

All cases underwent clinical examination and MPMRI with BOLD imaging on first follow up at 3 months. All post therapy MRI scans were reviewed by two radiologists. Absence of disease on MRI was categorized as “complete response” and the presence of residual disease as “partial response.” Second MPMRI with BOLD imaging was performed at 6 months. Further MRI imaging was performed only on clinical suspicion of residual or recurrent disease.

The radiologist was blinded to the clinical response and the radiation oncologist was blinded to the MPMRI with BOLD imaging findings. Conventional MRI was used by clinicians to evaluate response to therapy and plan further management. Response on conventional MRI was determined using T2-weighted images in sagittal and axial planes and calculating the residual tumor size. Pre and post therapy MPMRI and BOLD imaging findings were correlated and the changes in the parameter were analyzed to assess the response.

2.4. Statistical analysis

Statistical analysis was done to assess correlation between imaging parameters and pathologic diagnosis. All the relevant data were entered into SPSS version 16.0 data sheet for statistical computation. Agreement between the two radiologists was estimated by calculating κ and was interpreted as follows: 0.00–0.20, poor agreement; 0.21–0.40, fair agreement; 0.41–0.60, moderate agreement; 0.61–0.80, substantial agreement; and 0.81–1.00, almost perfect agreement [6]. The sensitivity, specificity, accuracy, positive predictive value and negative predictive value of MPMRI, were calculated using standard 2×2 tables, by comparing with the gold standard of final histopathology. Measures of diagnostic performance were estimated based on individual and combined

Table 2
Diffusion characteristics of the lesions.

Signal intensity on T2-weighted images	Signal intensity on exponential maps	Values on ADC maps	Interpretation of findings
Isointensity, hyperintensity	Hyperintensity	Decreased	High-cellularity recurrent tumour
Hypointensity, isointensity	Hypointensity	Decreased	Fibrous tissue/scar tissue
Hyperintensity	Hypointensity	Increased	Benign normal mucosa/inflammation/post therapy necrosis

Table 3
Diagnostic performance of conventional and MPMRI sequences in detecting recurrent lesions.

	Conventional MRI	MPMRI	Combined MRI	DCE	DWI	MRS	PD-IDEAL	BOLD
Sensitivity (%) (CI)	70.8 (48.7–86.5)	95.8 (76.8–99.7)	100 (82.8–100)	91.6 (71.5–98.5)	95.8 (76.8–99.7)	81.8 (58.9–94.0)	95.8 (76.8–99.7)	91.6 (71.5–98.5)
Specificity (%) (CI)	66.6 (24.1–94.0)	100 (51.6–100)	100 (51.6–100)	100 (51.6–100)	100 (51.6–100)	100 (19.7–100)	83.3 (36.4–99.1)	100 (51.6–100)
PPV (%) (CI)	89.4 (65.4–98.1)	100 (82.1–100)	100 (82.8–100)	100 (81.5–100)	100 (82.1–100)	100 (78.1–100)	95.8 (76.8–99.7)	100 (81.5–100)
NPV (%) (CI)	36.4 (12.3–68.3)	85.7 (42.0–99.2)	100 (51.6–100)	75.0 (35.5–95.5)	85.7 (42.0–99.2)	33.3 (6.0–75.8)	83.3 (36.4–99.1)	75.0 (35.5–95.5)
Accuracy	70	96.7	100	93.3	96.7	73.3	93.3	93.3

probability for correctly identifying the recurrence. Results were expressed as point estimates and their 95% CIs were derived from the binomial distribution. All *p*-values were two-tailed. *P*-value below 0.05 was considered significant. Statistical significance was also considered demonstrated if the 95% confidence intervals did not include zero.

3. Results

The mean diameter of soft-tissue nodules revealed at MRI was 1.5 cm (range, 0.7–4.8 cm). Based on the conventional imaging findings the lesions were categorized as: 11 in category 1 and 19 in category 2 and 3. The conventional and MPMRI appearances of lesions were analyzed and compared qualitatively. Statistical values of the conventional and MPMRI imaging tests are summarized in Table 3.

Combined qualitative and quantitative analysis of conventional MRI and MPMRI of the 11 patients in category 1, based on conventional sequences only, four were true negative and seven were false negative. These cases however were picked up as recurrence on MPMRI and showed restricted diffusion on DWI and hyperperfusion on quantitative color maps of DCE-MRI, suggestive of recurrence.

Similar analysis of 19 patients in category 2 and 3, based on conventional sequences only, two were false positive. These two cases showed T2 hyperintensity on conventional imaging with post-contrast enhancement however on MPMRI they had facilitated diffusion with hypoperfusion and no elevated choline peak.

The κ statistics agreement between the two radiologists for conventional MRI reading, MP-MRI reading and Combined MP-MRI images were 0.70, 0.65, and 0.69 respectively and the interobserver agreement was substantial.

3.1. MPMRI parameters

Statistical analyses of various MPMRI sequences are summarized in Table 3.

The DWI findings were compared to the T2W signal intensity of the lesion and are summarized in Table 2. A statistically significant difference in the ADC values was observed between the benign tissue and recurrent lesions ($p < 0.001$). Restricted diffusion was seen in 23 of the 24 cases and all the benign cases showed facilitated diffusion. We found that the median ADC (mADC) of recurrent carcinomas ($1.23 \pm 0.20 \times 10^{-3}$ mm^2/s) was significantly lower than benign vault tissue ($2.56 \pm 0.46 \times 10^{-3}$ mm^2/s) ($p < 0.001$).

Based on DCE- MRI, 22 cases showed findings suggestive of recurrence with no false positive cases and 8 cases showed hypoperfusion with 2 false negative cases. The recurrent lesions showed evidence of hyperperfusion with NEI of 354%. This was statistically higher than the values seen in benign cases (NEI of 76%, *p* value < 0.05).

1H-MRS was performed in 24 patients of which, 18 were positive for recurrence and showed significantly elevated choline. Two cases were benign and showed no elevated choline. There were four false negative cases. Spectroscopy could be performed in 6 cases because of the lesion was too small and had admixture of normal tissue in the spectroscopy voxel.

Based on the findings on PD-IDEAL imaging, suspicion of recurrence was raised in 24 cases and only one false positive case was documented.These lesions showed significant hyperintensity on WATER images and were hypointense on FAT images. 6 cases were diagnosed as benign on PD-IDEAL imaging which showed hypointensity on WATER images. There was one false negative case.

Qualitative and quantitative estimation of hypoxic fraction was performed using BOLD MRI. Of the 24 cases 22 had hypoxia on pretherapy MRI. Compared to benign fibrosis the recurrent lesions showed predominantly red maps representing higher R2* levels suggestive of higher concentration of deoxyhaemoglobin with a higher oxygen metabolism and very low tumor perfusion suggestive of chronic hypoxia (Figs. 3 and 4).

3.2. Follow up imaging to assess treatment response

Follow up imaging was performed in all the 24 recurrent cases to assess the therapy response. Of the 6 benign cases, 2 had one follow up MRI to check for local infection and showed no evidence of any disease after effective antibiotic therapy.

21 out of the 24 Post therapy follow-up MPMRI revealed significant increase in mADC values, with regression in the perfusion parameters of the lesion in 19 of the 22 cases and regression in the choline peak in 15 of the 19 cases. In 14 cases, correlation of combined all three parameters showed statistically significant correlation with response to therapy. We found a significant correlation between percentage tumor regression and pre-treatment parameters: NEI ($p = 0.02$), the maximum slope ($p = 0.04$) and mADC value ($p = 0.001$).

Of the 22 cases that showed significant intratumoral hypoxic fraction on BOLD imaging, 18 cases showed statistically interval regression in the hypoxic fractions and significant correlation between the tumor size reduction and the amount of hypoxia present in the pretherapy MRI ($p = 0.01$) Fig. 5.

Three lesions were found to be non-responsive to therapy on both multiparametric and BOLD MR imaging. One case showed significant increase in the mADC values on post therapy follow-up

however no significant change in the hypoxic fraction was noted in this case. In all the nonresponsive cases Pre-therapy BOLD imaging revealed a significantly large chronic hypoxic fraction which did not change statistically on post-therapy imaging. Overall the post therapy follow up MPMRI with BOLD hypoxia imaging parameters showed statistically significant correlation between the changes in tumor biology at at the molecular, subcellular, cellular and tissue levels (unavailable from routine structural imaging techniques alone) and response to therapy.

4. Discussion

Post-hysterectomy recurrence in patients with carcinoma cervix may involve the vaginal vault, parametrial tissue, urinary bladder and rectum. The occurrence of these recurrent lesions varies with the preoperative stage; histology of primary, extent of surgery and host response [7–10]. Most of these recurrences are asymptomatic however few patients may present with symptoms such as pain due to nerve compression, ureteric involvement or limb swelling due to lymphatic infiltration. Recurrence can be easily detected on routine clinical examination, surveillance CT, or MR imaging [7–10].

MRI is the standard imaging technique indicated for the initial evaluation of local spread (tumor size, spread to parametria, vagina, bladder, and rectum) and lymph node status in patients with cervical cancer [11,12,13]. One of the initial studies was by Hatano et al. and they reported a correlation between MRI and cytology and/or punch biopsy. The reported sensitivity, specificity, and negative and positive predictive values of MRI in their study was 100%, 78%, 43%, and 100%, respectively [12]. Another similar study by Nam et al., evaluated 38 patients treated with CRT and response evaluation done by MRI. They found 92% radiological response with local control rate of 100% in these patients [13].

Studies have shown that, similar to other tumors, carcinoma of the uterine cervix is associated with tumoral angiogenesis leading to abnormal contrast enhancement patterns [14,15]. Hawighorst et al. evaluated 24 patients with suspected cervical cancer recurrence using pharmacokinetic analysis of dynamic MR images. They found that the pharmacokinetic mapping of malignant lesions had a statistically significant shorter ($p < 0.005$) and stronger ($p < 0.001$) contrast medium enhancement ($t21$, 24 s; A, 1.5 arbitrary units) than that of benign lesions ($t21$, 65 s; A, 0.7). The test showed a sensitivity of 100%, a specificity of 88%, and an accuracy of 96% [15]. Similar results have been reported in Yamashita et al. study, performed to predict response to therapy based on DCE-MRI in patients with known cervical carcinoma [16]. The rate as well as the slope of enhancement has also been shown to correlate with local tumor control and outcome [17]. In our study, these differences were quantified and used to discriminate vaginal vault/local recurrence from postsurgical or residual fibrosis. We also found that post-therapy DCE-MRI has a role in predicting recurrence and identifying those who may benefit from salvage treatment.

DW imaging with ADC maps have been used to differentiate between benign and malignant cervical tissues and also to predict response to chemoradiotherapy on the basis of changes in the DW parameters in responders and non-responders [18]. Naganawa et al. showed statistically significant difference between the ADC values of benign and malignant cervical tissues. They reported mADC of cervical cancer tissue to be $1.09 \pm 0.20 \times 10^{-3}$ mm2/s while in normal cervix it wasfound to be $1.79 \pm 0.24 \times 10^{-3}$ mm^2/s ($p < 0.0001$) [19]. The mADC of cervical cancer was also shown to have significantly increased following chemoradiotherapy and the rapid increase in ADC values was shown to correlate with tumoral tissueapoptosis [20,21]. In our study DWI was found to be not only helpful in diagnosing recurrent disease but also has potential to predict response to therapy.

Studies have reported an important limitation of 1HMRS imaging in cervical cancer patients. There is significant spectral contamination on MR spectra on evaluation of small tumors which are less than 8 mm leading to inconclusive results [22,23]. Recent studies have shown that 1H-MRS can distinguish preinvasive cervical cancers from early invasive lesions. It has also been shown to help in predicting response to radiotherapy/neoadjuvant chemotherapy and survival outcome [24,25]. To the best of our knowledge there is no literature available on the diagnostic value of MR spectroscopy for detection of vault/local recurrence after radical hysterectomy. In our series we could perform 1H-MRS in 80% of patients with sensitivity of 81.8% and specificity of 100%.

BOLD hypoxia imaging is a promising tool to analyze vascular functionality associated with angiogenesis [26]. It uses deoxyhaemoglobin as an intrinsic paramagnetic contrast agent and is found to be sensitive to changes in blood volume, blood flow and blood oxygenation [27,28]. Preliminary results of Kim et al. study suggested that BOLD imaging at 3-T MRI is an important imaging biomarker and in future it may have the potential to response assessment in cervical cancer patients [29,30]. In our study we found that the tumor maps of BOLD shows three zone of hypoxia spectra with central core representing chronic hypoxia [30]. This zone showed significant correlation with response assessment on follow up BOLD imaging. We found that estimating the central core volume could be a prognostic marker for predicting response to therapy.

To conclude, there are existing studies assessing the role of individual MPMRI parameter in evaluating tumoral microenvironment but to our knowledge, the current study is the first to correlate all the MPMRI with BOLD hypoxia imaging parameters with histology for recurrent cervical cancer. Furthermore, all patients had received the same treatment modalities and had a histopathological diagnosis which was the gold standard. However, larger studies are warranted to further establish the role of MPMRI and BOLD hypoxia imaging in evaluation of the post-operative recurrent cervical cancers.

5. Conclusion

In our experience, conventional MR with MPMRI imaging significantly increases the diagnostic accuracy for suspected vaginal vault/local recurrence with nearly 100% correlation with histopathological findings. Therefore, dedicated MPMRI should be applied when there is clinical suspicion of recurrence. Post therapy serial MPMRI with BOLD hypoxia imaging follow-up objectively documents the response. MPMRI and BOLD hypoxia imaging provide information regarding tumor biology at the molecular, subcellular, cellular and tissue levels and this information may be used as an appropriate and reliable biologic target for radiation dose painting to optimize therapy in future.

Conflict of interest

None.

Authors contributions

Guarantors of integrity of entire study, A.M, M.H.T; study concepts/study design or data acquisition or data analysis/interpretation, all authors; manuscript drafting or manuscript revision for important intellectual content, all authors; manuscript final version approval, all authors; literature research, all authors;

clinical studies, A.M, S.C, R.E; statistical analysis, A.M, S.C, U.M; and manuscript editing, all authors.

Dr. Mahajan had full access to all of the data in the study and takes responsibility for the integrity of the data and the accuracy of the data analysis.

Financial disclosures

None.

Funding/support

None.

Role of the sponsor

Not applicable.

Acknowledgements

I am extremely grateful to Dr Vicky Goh, MD, FRCR and Dr Richa Vaish Mahajan, MBBS, MS for their valuable inputs.

References

[1] N. Colombo, S. Carinelli, A. Colombo, C. Marini, D. Rollo, C. Sessa, ESMO Guidelines Working Group, Cervical cancer: ESMO clinical practice guidelines for diagnosis, treatment and follow-up, Ann. Oncol 7 (Suppl. 23) (2012) vii27–vii32.

[2] S.A. Cannistra, J.M. Niloff, Cancer of the uterine cervix, N. Engl. J. Med. 334 (1996) 1030–1037.

[3] C. Meads, C. Davenport, S. Małysiak, M. Kowalska, A. Zapalska, P. Guest, et al., Evaluating PET-CT in the detection and management of recurrent cervical cancer: systematic reviews of diagnostic accuracy and subjective elicitation, BJOG 121 (2014) 398–407.

[4] T.M. Weber, H.D. Sostman, C.E. Spritzer, R.L. Ballard, G.A. Meyer, D.L. Clark-Pearson, J.T. Soper, Cervical carcinoma: determination of recurrent tumor extent versus radiation changes with MR imaging, Radiology 194 (1995) 135–139.

[5] H. Hricak, P.S. Swift, Z. Campos, J.M. Quivey, V. Gildengorin, H. Göranson, Irradiation of the cervix uteri: value of unenhanced and contrast-enhanced MR imaging, Radiology 189 (1993) 381–388.

[6] J.R. Landis, G.G. Koch, The measurement of observer agreement for categorical data, Biometrics 33 (1977) 159–174.

[7] D. Bodurka-Bevers, M. Morris, P.J. Eifel, C. Levenback, M.W. Bevers, K.R. Lucas, J.T. Wharton, Posttherapy surveillance of women with cervical cancer: an outcomes analysis, Gynecol. Oncol. 78 (2000) 187–193.

[8] L. Elit, A.W. Fyles, M.C. Devries, T.K. Oliver, M. Fung-Kee-Fung, C. Gynecology, D. ancer, S. isease, G. ite, roup, Follow-up for women after treatment for cervical cancer: a systematic review, Gynecol. Oncol. 114 (2009) 528–535.

[9] Y.Y. Jeong, H.K. Kang, T.W. Chung, J.J. Seo, J.G. Park, Uterine cervical carcinoma after therapy: CT and MR imaging findings, Radiographics 23 (2003) 969–981, discussion 981.

[10] L.L. Subak, H. Hricak, C.B. Powell, L. Azizi, J.L. Stern, Cervical carcinoma: computed tomography and magnetic resonance imaging for preoperative staging, Obstet. Gynecol. 86 (1995) 43–50.

[11] J.I. Choi, S.H. Kim, C.K. Seong, J.S. Sim, H.J. Lee, K.H. Do, Recurrent uterine cervical carcinoma: spectrum of imaging findings, Korean J. Radiol. 1 (2000) 198–207.

[12] K. Hatano, Y. Sekiya, H. Araki, M. Sakai, T. Togawa, Y. Narita, et al., Evaluation of the therapeutic effect of radiotherapy on cervical cancer using magnetic resonance imaging, Int. J. Radiat. Oncol. Biol. Phys. 45 (1999) 639–644.

[13] H. Nam, W. Park, S.J. Huh, D.S. Bae, B.G. Kim, J.H. Lee, et al., The prognostic significance of tumor volume regression during radiotherapy and concurrent chemoradiotherapy for cervical cancer using MRI, Gynecol. Oncol. 107 (2007) 320–325.

[14] K. Kinkel, M. Ariche, A.A. Tardivon, A. Spatz, D. Castaigne, C. Lhomme, et al., Differentiation between recurrent tumor and benign conditions after treatment of gynecologic pelvic carcinoma: value of dynamic contrast-enhanced subtraction MR imaging, Radiology 204 (1997) 55–63.

[15] H. Hawighorst, P.G. Knapstein, U. Schaeffer, M.V. Knopp, G. Brix, U. Hoffmann, et al., Pelvic lesions in patients with treated cervical carcinoma: efficacy of pharmacokinetic analysis of dynamic MR images in distinguishing recurrent tumors from benign conditions, AJR Am. J. Roentgenol. 166 (1996) 401–408.

[16] J.H. Kim, C.K. Kim, B.K. Park, S.Y. Park, S.J. Huh, B. Kim, Dynamic contrast-enhanced 3-T MR imaging in cervical cancer before and after concurrent chemoradiotherapy, Eur. Radiol. 22 (2012) 2533–2539.

[17] W.T. Yuh, N.A. Mayr, D. Jarjoura, D. Wu, J.C. Grecula, S.S. Lo, et al., Predicting control of primary tumor and survival by DCE MRI during early therapy in cervical cancer, Invest. Radiol. 44 (2009) 343–350.

[18] F. Kuang, J. Ren, Q. Zhong, F. Liyuan, Y. Huan, Z. Chen, The value of apparent diffusion coefficient in the assessment of cervical cancer, Eur. Radiol. 23 (2013) 1050–1058.

[19] S. Naganawa, C. Sato, H. Kumada, T. Ishigaki, S. Miura, O. Takizawa, Apparent diffusion coefficient in cervical cancer of the uterus: comparison with the normal uterine cervix, Eur. Radiol. 15 (2005) 71–78.

[20] H.S. Kim, C.K. Kim, B.K. Park, S.J. Huh, B. Kim, Evaluation of therapeutic response to concurrent chemoradiotherapy in patients with cervical cancer using diffusion-weighted MR imaging, J Magn. Reson. Imaging 37 (2013) 187–193.

[21] K. Downey, S.F. Riches, V.A. Morgan, S.L. Giles, A.D. Attygalle, T.E. Ind, et al., Relationship between imaging biomarkers of stage I cervical cancer and poor-prognosis histologic features: quantitative histogram analysis of diffusion-weighted MR images, AJR Am. J. Roentgenol. 200 (2013) 314–320.

[22] S.J. Booth, M.D. Pickles, L.W. Turnbull, In vivo magnetic resonance spectroscopy of gynaecological tumours at 3.0 Tesla, BJOG 116 (2009) 300–303.

[23] J.R. Allen, R.W. Prost, O.W. Griffith, S.J. Erickson, B.A. Erickson, In vivo proton (H1) magnetic resonance spectroscopy for cervical carcinoma, Am. J. Clin. Oncol. 24 (2001) 522–529.

[24] M.M. Mahon, I.J. Cox, R. Dina, W.P. Soutter, G.A. McIndoe, A.D. Williams, et al., (1)H magnetic resonance spectroscopy of preinvasive and invasive cervical cancer: in vivo-ex vivo profiles and effect of tumor load, J. Magn. Reson. Imaging 19 (2004) 356–364.

[25] N.M. deSouza, W.P. Soutter, G. Rustin, M.M. Mahon, B. Jones, R. Dina, et al., Use of neoadjuvant chemotherapy prior to radical hysterectomy in cervical cancer: monitoring tumour shrinkage and molecular profile on magnetic resonance and assessment of 3-year outcome, Br. J. Cancer 90 (2004) 2326–2331.

[26] V. Tóth, A. Förschler, N.M. Hirsch, J. den Hollander, H. Kooijman, J. Gempt, et al., MR-based hypoxia measures in human glioma, J. Neurooncol. 115 (2013) 197–207.

[27] N.M. Hirsch, V. Toth, A. Förschler, H. Kooijman, C. Zimmer, C. Preibisch, Technical considerations on the validity of blood oxygenation level-dependent-based MR assessment of vascular deoxygenation, NMR Biomed. 27 (July (7)) (2014) 853–862.

[28] L. Jiang, P.T. Weatherall, R.W. McColl, D. Tripathy, R.P. Mason, Blood oxygenation level-dependent (BOLD) contrast magnetic resonance imaging (MRI) for prediction of breast cancer chemotherapy response: a pilot study, J. Magn. Reson. Imaging 37 (2013) 1083–1092.

[29] C.K. Kim, S.Y. Park, B.K. Park, W. Park, S.J. Huh, Blood oxygenation level-dependent MR imaging as a predictor of therapeutic response to concurrent chemoradiotherapy in cervical cancer: a preliminary experience, Eur. Radiol. 24 (July (7)) (2014) 1514–1520.

[30] A. Mahajan, V. Goh, S. Basu, R. Vaish, A.J. Weeks, M.H. Thakur, G.J. Cook, Bench to bedside molecular functional imaging in translational cancer medicine: to image or to imagine? Clin. Radiol. 70 (July 15) (2015), http://dx.doi.org/10.1016/j.crad.2015.06.082, pii: S0009-9260(15). [Epub ahead of print] Review. PubMed PMID: 26187890.